

# **NANO ENGINEERED SELF SENSING CONCRETE FOR SMART STRUCTURES**



## **FINAL YEAR PROJECT UG 2017**

By

Muhammad Hanzla Razaqat	237531
Muhammad Faisal Rauf	209879
Ahmad Naseem	216529

NUST Institute of Civil Engineering  
School of Civil and Environmental Engineering  
National University of Sciences and Technology, Islamabad,  
Pakistan

2021

This is to certify that the  
Final Year Project Titled

**“NANO ENGINEERED SELF SENSING CONCRETE FOR  
SMART STRUCTURES”**

Submitted by

Muhammad Hanzla Razaqat	237531
Muhammad Faisal Rauf	209879
Ahmad Naseem	216529

has been accepted towards the requirements  
for the undergraduate degree

**in**

**CIVIL ENGINEERING**

---

Dr. Hammad Anis Khan  
Associate Professor NICE NUST  
NUST Institute of Civil Engineering  
School of Civil and Environmental Engineering  
National University of Sciences and Technology, Islamabad, Pakistan

## ACKNOWLEDGEMENTS

In the name of Allah, the most merciful, the most beneficent, all praise to Him, the lord of the worlds and all prayers and Hazrat Muhammad (S.A.W), his servant and final messenger.

We are, first of all, grateful to Almighty Allah; without Whose willingness and blessings, we would have never achieved what we have ended up ultimately accomplishing.

We would like to show appreciation to our beloved parents and teachers for their unconditional love and encouragement throughout our lives and for supporting us in realizing our dreams.

Our journey of BSc, especially our thesis year, has been a remarkable experience for all of us, and we cannot be more thankful to all people who were a part of this journey with us. We find ourselves at a loss for words to express our gratitude to all the people who motivated, encouraged, advised, and helped us complete this journey.

At the outset, we would like to express our appreciation to our supervisor Dr. Hammad Anis Khan, for his constant mentorship throughout this journey. He remained a source of rare and valuable advice for us during this endeavor for more than a year. He has constantly motivated us to remain focused on achieving our goals. His expertise was integral in helping us demarcate the direction of our research and moving forward with the investigation in depth. His inexorable support immensely helped us during our research and investigation period and enhanced our scientific writing skills. Our sincerest and heartfelt thanks to him for helping us to become hard-working, knowledgeable, and better people.

We would also like to express our gratitude to Dr. Khurram Yaqoob, Associate Professor, SCME, NUST, for facilitating us in various tests performed in SCME. We would also like to thank the lab staff of different labs, especially Structural Lab NICE, for assisting us in various tests.

We are grateful to the P.G. students of NICE, Ms. Anum, and Nafeesa, for carving out time from their work to guide us with the trial testing and the methods to optimize our results and testing. Special thanks to Ms. Meshwish Khalid of Microbiology Lab (IESE, NUST) for her assistance and valuable support.

Special thanks to Dr. Zafar (Vice-Chancellor UoT Nowshehra) for assisting us in the procurement of nano-particles. We want to express our gratitude to Dr. Habib Bokhari (Vice-Chancellor Kohsar University, Murree) for providing us with the qualitative chemical agents used in our experimentation.

# *Dedication*

To

*Our Advisor Dr. Hammad Anis Khan*

&

*Our Families and Friends*

## **ABSTRACT**

This study aims to design a multifunctional cement composite that can bear loads and possess electromechanical properties by integrating structural health monitoring (S.H.M.) systems within the concrete. Traditionally, dispersive conductive fillers were a common technique utilized. However, this process was costly and involved complex variables challenging and affecting structural integrity. We aim to leverage this approach's weakness and introduce a new S.H.M. technique in which carbon fiber-based ink solution is sprayed on the cement-aggregate interface, which is less costly and offers less complex dispersion. A well-defined conductive network was established on the spray's drying, forming electrically conductive, thin film-coated aggregates. The thin film-coated aggregates were used to cast multiple concrete cylinders and beam specimens to validate conductivity and concrete's mechanical properties. It was demonstrated experimentally that this procedure yielded specimens that showed better conductivity and had electrical properties that varied in response to applied loads, successively detecting damage locations and their severities in the structure even before damage being detected with the naked eye, which propagated rapidly, causing sudden failures. Thus, our process enabled the self-sensing properties of the film, enhancing the concrete within a budget while limiting the challenging variables associated with the previous technique.

## Table of Contents

LIST OF FIGURES .....	10
LIST OF TABLES.....	11
LIST OF NOTATIONS .....	12
CHAPTER 1 .....	13
INTRODUCTION .....	13
1.1 General Overview .....	13
1.2 Self-Sensing .....	13
1.3 Problem Statement .....	14
1.4 Objectives .....	14
1.5 Thesis Structure .....	15
CHAPTER 2 .....	16
LITERATURE REVIEW .....	16
2.1 Self-Sensing .....	16
2.1.1 External Techniques.....	16
2.1.2 Flaws Identification .....	17
2.1.3 Self-Sensing Technique .....	17
2.1.4 Potential and past researched self-sensing materials .....	17
2.2 Carbon fibers and carbon nanotubes.....	17
2.2.1 Dispersion of carbon nanocomposites in cementitious matrices .....	18
2.2.2 Carbon Nano-particles .....	19
2.3 Percolation Threshold Theories .....	21
2.3.1 IPD (Inter particle distance) approach .....	22
2.3.2 Celzard approach .....	22

2.3.3 Ratio approach for percolation threshold.....	22
2.4 Research Gap .....	23
CHAPTER 3 .....	24
MATERIALS AND EXPERIMENTAL METHODOLOGY .....	24
3.1 Materials .....	24
3.1.1 Nano Material - Carbon Nano-particles (CNPs):.....	24
3.1.2 N-Methyl-2-pyrrolidone (NMP) .....	25
3.1.3 Poly sodium 4-styrene Sulfonate (PSS).....	25
3.1.4 Polyvinylidene Fluoride (PVDF).....	27
3.1.5 Cement (Bestway).....	28
3.1.6 Fine Aggregate.....	28
3.1.7 Coarse Aggregate.....	29
3.1.8 Mixing Water .....	29
3.2 Experimental Methodology .....	30
3.2.1 Optimum Proportion & Sonication.....	32
3.2.2 Mix Design.....	34
3.2.3 Mixing Regime .....	34
3.2.4 Slump Test .....	35
3.2.5 Curing Process .....	36
CHAPTER 4.....	37
EXPERIMENTAL TESTS AND RESULTS .....	37
4.1 Modulus of Rupture (MoR) .....	37
4.2 Compressive Strength .....	38
4.3 Bulk Resistivity.....	40
4.4 Self-Sensing .....	42
4.4.1 Test setup and procedure .....	42



4.4.2 Piezoresistive Test – Damage Sensing (DS).....	42
CHAPTER 5 .....	45
CONCLUSIONS.....	45
RECOMMENDATIONS .....	46
REFERENCES .....	47

## LIST OF FIGURES

Figure 1: Formation of effective conductive network with increasing filler concentration .....	21
Figure 2: SEM image of Carbon Nano Particles at 500 nm scale .....	25
Figure 3: SEM of PSS at 0.5 $\mu\text{m}$ and 20 $\mu\text{m}$ scale .....	26
Figure 4: SEM of PVDF at 0.5 $\mu\text{m}$ and 5 $\mu\text{m}$ scale .....	27
Figure 5: Particle Size Distribution of Sand .....	28
Figure 6: Ink Fabrication Process .....	30
Figure 7: Preparation of CNP based ink .....	31
Figure 8: Addition of CNP Solution to Mix design .....	31
Figure 9: Coarse aggregate before and after coating .....	32
Figure 10: Fine aggregates before and after spray .....	32
Figure 11: Sonication in Progress, Glass test tubes having different proportions .....	33
Figure 12: Spectrophotometer, Peak Detection Values .....	33
Figure 13: Slump (Control, CNP as additive, CNPs Sprayed) .....	35
Figure 14: Modulus of rupture values .....	37
Figure 15: Compressive Strength Test Cylinder in UTM .....	38
Figure 16: Compressive strengths and comparison with MoR .....	39
Figure 17: Bulk Resistivity Test .....	40
Figure 18: Bulk Resistivity Test Result .....	41
Figure 19: Piezoresistive Testing apparatus Setup .....	43
Figure 20: Resistivity vs. Load trend in damage sensing .....	44

## LIST OF TABLES

Table 1: Cement properties.....	28
Table 2: Different properties of sand.....	29
Table 3: Different properties of aggregate .....	29
Table 4: Trials for optimum proportion of solution constituents .....	34
Table 5: Mix Design .....	34
Table 6: Execution steps of casting .....	35

## LIST OF NOTATIONS

ASTM	American Society of Testing and Materials
SHM	Structural Health Monitoring
PSA	Particle Size Analysis
SEM	Scanning Electron Microscopy
EDS	Energy Dispersive Spectroscopy
OM	Optical Microscopy
UVS	Ultraviolet Spectroscopy
DDF	Ductility Deformation Factor
EPT	Elastic-Plastic Toughness
MoR	Modulus of Rupture
CWMA	Crack Width Measurement Analysis
SRI	Strength Recovery Index
DS	Damage Sensing
SS	Strain Sensing
PVDF	Polyvinylidene fluoride
PSS	Poly sodium 4- styrene sulfonate
CNPs	Carbon Nano Particles
NMP	N-methyl-2-pyrrolidone
UPV	Ultrasonic Pulse Velocity

# CHAPTER 1

## INTRODUCTION

### 1.1 General Overview

Concrete is the most widely used construction material in the world due to its versatile characteristics like formlessness, plasticity, hydraulicity, strength, and toughness and is relatively cheap. However, since it is predominantly brittle in nature and has a low tensile strength, it is susceptible to progression and coalescence in micro-cracks, rendering low strength and durability (Khaliq et al., 2016). Progression and the corresponding increase in width of cracks can cause them to house deleterious substances that can also be detrimental to concrete durability. It is estimated that the damages due to the corrosion of concrete in the US are \$276 billion (Koch et al., 2002), with the annual cost in repairs to be \$18 – 21 billion per year (Emmons and Sordyl, 2006). And prior to the repair applied, structures also require periodic maintenance, i.e., Structural Health Monitoring (SHM), which also carries a significant cost. Therefore, it is imperative to develop intrinsic monitoring in the cementitious matrix to detect the propagation of such cracks. There is a compelling economic incentive to develop a multipurpose Nano-engineered Concrete Composite that can sense damage all by itself.

### 1.2 Self-Sensing

Self-sensing involves microstructural modification of cementitious matrix by addition of conductive filler whose conductive properties can be utilized to monitor such deteriorations produced at nano and micro levels, also termed Structural Health Monitoring (SHM). SHM in such type of smart modified cementitious matrix with self-sensing properties can be applied to check the depth of cracks produced inside the structure by keeping the record of its resistivity with respect to the applied current (Lu, Xie, Feng, & Zhong, 2015).

### **1.3 Problem Statement**

In the past, numerous studies have been conducted to develop self-sensing concrete that utilizes the electrical resistance of concrete to detect micro-cracks before they are visible to the human eye. For this purpose, numerous materials have been incorporated in the concrete mix to enhance the electrical properties of the concrete mix. It has been noticed that the conductivity of concrete depends on two factors; first, the conductivity of the filler itself, and second, the ability of the filler to form a well-defined conductive path. However, due to the ability of nano-particles to agglomerate, it is difficult to disperse them to reduce resistivity effectively. Most of these nanocomposites used as fillers, like CNTs, are expensive; therefore, their use in the construction industry is limited, demanding economically viable products. Keeping these points in view, a new technique is used, which is relatively easy, cheaper, and effective. This technique utilizes carbon nano-particles (CNPs) in latex polymer to make conductive ink. (Gupta, 2016) which is sprayed onto the aggregate surface to create conductive concrete. As in this technique, aggregates are nano-engineered; hence a well-defined conductive path is already formed because of the dense network of aggregates. Also, since the ink is to be sprayed, the quantity of nano-material required is drastically reduced to about 0.005% of the cement used.

### **1.4 Objectives**

In light of components detailed out in the problem statement, the objectives of our thesis are enlisted as follows:

1. To achieve conductivity in concrete through the addition of Carbon Nano Particles (CNPs) in the concrete mix using an airbrushing technique.
2. To formulate a conductive ink by carrying out trial testing and studying correlation and effectiveness of utilizing different concentrations of CNPs, N-methyl-2-pyrrolidinone (NMP) and Polystyrene sulfonate (PSS).

3. To compare the conductivity in concrete using the conventional technique in which the conductive ink is added directly to the concrete mix with the airbrushing technique
4. To perform a comparative study of electrical resistivity of nano-modified conductive concrete, additive conductive concrete, and control concrete.
5. To perform a comparative study of mechanical properties of nano-modified conductive concrete, additive conductive concrete, and control concrete.
6. To evaluate changes in the resistivity by damage sensing for Structural Health Monitoring (SHM) applications.

## **1.5 Thesis Structure**

Following this introductory chapter, a literature review on self-sensing and self-sensing materials is presented in Chapter 2.

Chapter 3 describes the experimental research methodology, testing procedures, and materials used in casting. Mix design, casting regime, and curing have also been discussed in this chapter.

Chapter 4 includes tests conducted in different samples cast and their results. It outlines a detailed analysis of self-sensing of different samples, and its results are also discussed in this chapter. Also, a comparison of electromechanical properties of the three mix designs is carried out in the same chapter.

Conclusions based on the findings of this research and future recommendations are presented in Chapter 5.

## CHAPTER 2

### LITERATURE REVIEW

#### 2.1 Self-Sensing

The process of executing damage detection and formulating the corresponding characterization strategy for civil engineering structures is known as a structural health monitoring system (SHM).

Hence the starting point for developing an SHM system is to introduce a level of structural sensing capability that is both reliable and has long-term sustainability (M. Sun et al., 2009). In order to detect the damage, two main strategies can be adopted. The first being external, whereas the second being internal (material property based).

##### 2.1.1 External Techniques

There are two further main strategies in this category, the first being visual inspection, which is currently under practice. However, as it is experience-based and is a qualitative approach, it lacks the sophistication to detect and analyze internal and minor damage. The second strategy is related to NDE (Non-destructive evaluation), which includes static-based and vibration-based testing. Some of the techniques employed in NDE include (Dr. Khoushik Roy et al., 2016):

- a. Radiography
- b. Strain gauges
- c. Thermal infrared test
- d. Eddy current test
- e. Magnetic particle testing
- f. Ultrasonic test



### **2.1.2 Flaws Identification**

However, with time and progress, it was identified that even basic strain gauges or any other pressure sensor already proves to be quite expensive, so if we move towards increased sensitivity, it would be highly uneconomical. On the other hand, these instrumentations require prior knowledge of potential damage region, as well as each module has a limited zone of influence, so coverage of larger area requires greater number of modules which makes it expensive (Moubray, J. 1997).

### **2.1.3 Self-Sensing Technique**

Based on the limitations identified, the latest advancement is being done in the self-sensing domain with the aim of catering to these issues. The concept is to self-equip the material that is to be utilized for the construction of the structure with the ability to sense the damage incurred (Diego L. 2021).

### **2.1.4 Potential and past researched self-sensing materials**

The most common principle being utilized in the self-sensing domain is piezo resistivity that is response of resistivity of material to pressure applied on it. So for a material to be utilized in a cementitious composite, it has to possess electrical conductive properties and must have nano/micro-sized particles to effectively fill the cementitious matrix to form the desired conductive network and have a positive impact on the physical properties of the compound product. Based on these requirements, few materials have been researched so far (Nauman S. 2021).

## **2.2 Carbon fibers and carbon nanotubes**

Carbon nanotubes (CNTs) are graphite-based allotropes of carbon form enveloped into a cylindrical tube. The diameter of CNTs ranges between 2 and 100 nanometers, whereas carbon fibers (CFs) have a diameter ranging from 5 -10 microns (Iijima, 1991). It has been established that the ideal percolation threshold range for CFs to form an adequate piezoresistive sensor is from 0.5 to 1.0 % volume of the cement paste. Whereas for multi-walled carbon nanofibers (MWCNTs), 1.0 % by volume of cement paste was identified as the optimum value. A hybrid composite of both MWCNTs and CFs proves to be twice as

expensive in order to get the same results as of 1.0 vol.% MWCNTs (Dr. Seung Jung Lee et al., 2017).

However, CNTs are described as the best conductive material due to their high aspect ratio. Their nano size, as well as high aspect ratio, helps to improve the mechanical and electrical properties of the composite.

### **2.2.1 Dispersion of carbon nanocomposites in cementitious matrices**

Dispersion is the process of breaking down clusters formed due to the development of attractive electrostatic forces between individual particles. Proper dispersion of carbon nano-materials in cementitious matrices is a major concern that directly affects cement-based nanocomposites' properties. It is not feasible to directly disperse nano/micro composites within cement paste. Dispersion of nano materials must be homogeneous to create a conductive network to reduce the resistivity of the concrete. However, the property of nano-materials to agglomerate due to the large surface area, high aspect ratio, and strong Vander Waal's forces lead to a less efficient network. (K.M. Liew, 2016).

Several methods for properly dispersing CNTs have been developed in the last couple of years, divided into physical and chemical methods. Sonication, ball milling, and mechanical stirring are examples of physical methods, whereas chemical methods include using various surfactants to disperse CNTs. Sonication disperses CNT agglomerations by providing energy to overcome Van der Waals (VdW) interactions. Voltage is converted into pressure waves, which create a cavitation field and produce microbubbles. These will break the bonding between the fibers. Ball milling and mechanical steering or shear mixing will break the VdW interactions but cannot disperse CNTs properly. These methods are usually used as a preliminary treatment or in conjunction with sonication.

With chemical methods, covalent or noncovalent bonds are added to improve the wettability of the CNTs surface. Chemical methods are used to improve the wettability of CNT surfaces by adding covalent or noncovalent bonds. Adding polar functionalized groups such as carboxyl (COOH) to the surface of CNTs is a common way to form covalent bonds. Another technique is to grow polymer chains from CNT surfaces, which keeps the CNTs at a distance and improves wettability. Surfactants can be used to disperse CNTs, resulting in polymer chains.

Combinations of the aforementioned methods, such as ultrasonication and surfactants, are used to disperse CNTs in current experimental research. A diagram of how the mixing process would take place using surfactants, a magnetic stirrer, and ultrasonication to disperse CNTs properly is shown in Figure 6. First, a surfactant such as a superplasticizer is added to water. Pure CNTs are poured into the liquid solution with this solvent. The surfactant aids in dispersing the CNTs, but the fibers will be dispersed very uniformly by mixing the solution with a magnetic stirrer and sonication.

In the following, the use of surfactants will be further discussed. Through VdW forces, CNTs absorb the hydrophobic part of the added surfactant at the sidewalls, while aqueous solubility and electrostatic repulsion ensure fiber distribution. The density of polymers on the CNT's surface determines the range and strength of electrostatic repulsion. The optimal surfactant/CNT mass ratio varies depending on the type of surfactants and CNTs used. Surfactants that negatively affect the hydration process should not be used because they react with the cement hydrates. Surfactants with a similar structure, such as superplasticizers, are preferred because superplasticizers are already widely used in the cement industry. Because of the extremely high specific surface area of MWCNTs, the amount of water and superplasticizer must be slightly increased (Azhari & Banthia, 2012). To achieve good results for MWCNT dispersion, the amount of superplasticizer in a mixture was 0.023 – 0.14 percent by weight of water in a mixture (Liew et al., 2016). CNTs behave exceptionally well on the mechanical and electrical properties of cement-based composites when they are well-dispersed.

### **2.2.2 Carbon Nano-particles**

Cement composites with enhanced electrical characteristics have shown promise as structural deformation sensors in recent years. The influence of carbon nano-particles on the cement hydration process and the high dispersion of conductive particles explain the decrease in the electrical resistivity of concrete caused by their use. With the addition of CNPs, the nature of porosity changes in increasing the number of small micropores, resulting in a dense hardened cement paste with a more uniform distribution of nanosized conductive particles. This creates a homogeneous microstructure of electrically conductive concrete.

The electrical resistance of concrete is proven to halve with the addition of CNP in a small amount compared to the known electrically conductive additives such as graphite and carbon black, giving it a more durable structure of the concrete matrix (Artamonova, 2017). Carbon conductive additives are known to form continuous conductive chains in electrically conductive concrete; however, when their concentration is high, the strength of the concrete is reduced. Continuous conductive chains are formed when carbon nanoparticles are used, but due to the high specific resistance of CNP particles and their uniform distribution in concrete, it decreases the material's electrical resistance.

The study of the compressive strength of hardened cement paste with various concentrations of carbon nano-particles revealed that higher results were obtained with a CNP content in the range of 0.01–0.1 wt. percent, with a 30–35 % improvement in strength compared to the control specimen, which was accounted for by increased density of the microstructure (Urkhanova L. 2019). During the curing process, a greater number of pores in the control composition are filled with lime crystals of  $\text{Ca(OH)}_2$ . The addition of CNPs reduces capillary porosity, increasing the number of tiny gel pores in the calcium silicate hydrogel. There is a dense micro reinforcement and its binding to additional calcium hydro silicates in the formed portlandite's contact zone, which leads to an increase in the composite's density and strength.

## 2.3 Percolation Threshold Theories

Percolation threshold is a mathematical term related to percolation theory, which identifies the minimum content of filler required to be added to form a desired conductive network inside the cementitious matrix. Theoretical evaluation of the percolation threshold range will be evaluated using different mathematical models. However, to verify these theoretical percolation threshold ranges and establish an experimental percolation threshold range, samples have to be cast, and their electrical conductivity has to be tested via a 4-probe test. In literature, some relations are derived based on empirical methods and numerical simulations used to estimate the percolation threshold of CNPs in cement composites.

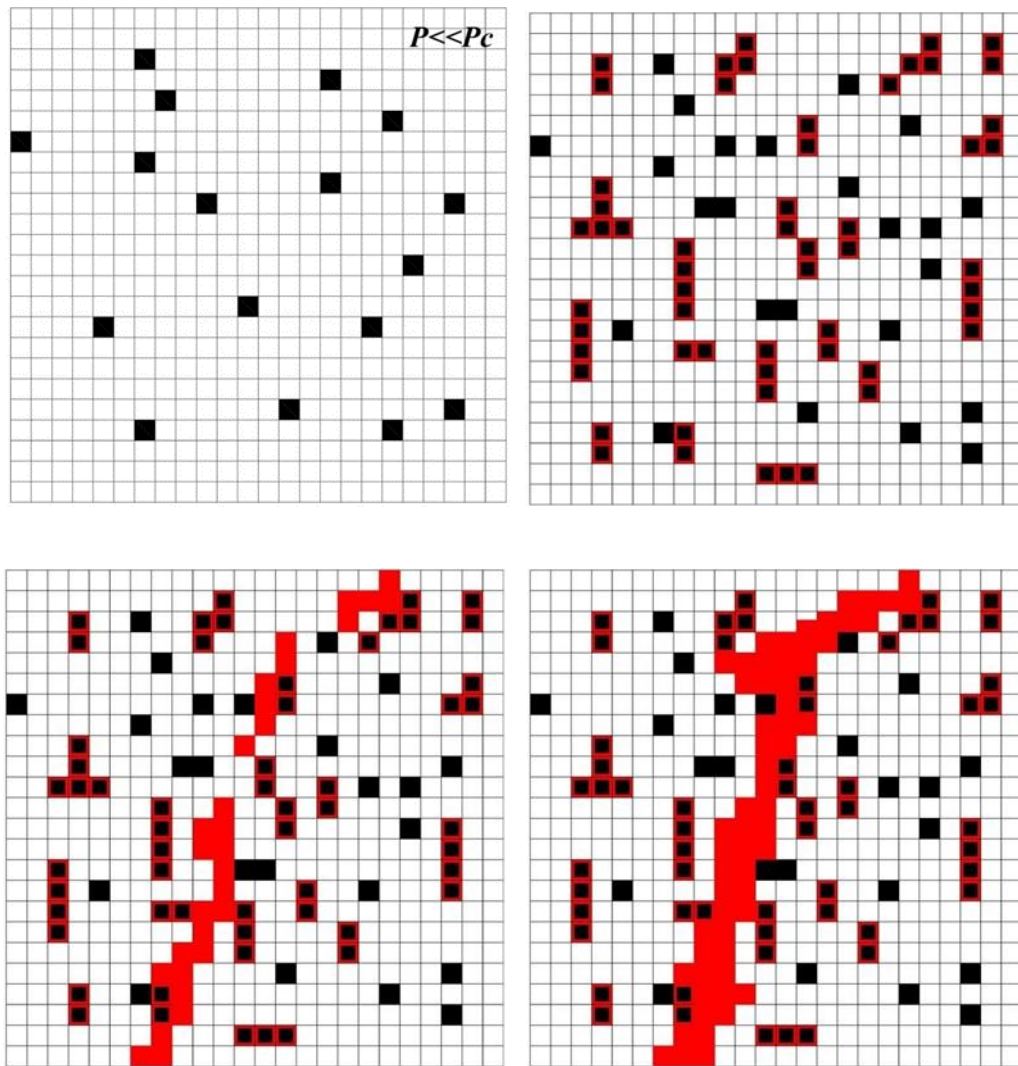


Figure 1: Formation of effective conductive network with increasing filler concentration

### 2.3.1 IPD (Inter particle distance) approach

It is a mathematical model that utilizes IPD and aspect ratio of individual particles of disc-shaped nanosized platelets in polymer composites proposed by Jing li et. al.. The equation for the model is:

$$P_c = \frac{27\pi D^2 t}{4(D + IPD)}$$

The mechanism of electron hopping is initiated if IPD is less than or equal to 10nm. Since IPD is very small in comparison with the average effective diameter D of nanoplatelets, it may be ignored, and finally, the equation reduces to:

$$P_c = \frac{27\pi t}{4D} = \frac{21.195}{\alpha}$$
$$\alpha = \frac{D}{t}$$

However, this model tends to give exaggerated values based on observation of related studies leading to uneconomical results.

### 2.3.2 Celzard approach

Celzard.et al. proposed a relation for percolation threshold related to the aspect ratio of conductive fillers, which is based on excluded volume approach and is as follows;

$$P_c = 1 - \exp\left(-\frac{3.6t}{\pi D}\right) \leq \phi_c \leq 1 - \exp\left(-\frac{5.6t}{\pi D}\right)$$

Where D denotes the diameter of individual CNP and t is its thickness (lesser dimension)

### 2.3.3 Ratio approach for percolation threshold

Celzard.et al. also proposed a relation for percolation threshold based on C:S (cement-sand ratio) and water-cement ratio. The resulting mathematical equation for the model is as follows:

$$P_c = 0.36 * \left(\frac{c + s + w}{c + s}\right)$$

## **2.4 Research Gap**

We deduced that to enhance the sensitivity of the concrete by imparting nano-engineered ink, we had to first dive into the research and investigate the morphology of the materials used to augment the behavior of each material used with respect to each other. Also, the quantities of each material used had to be first checked through literature and then confirmed through trial testing. Hence, the materials used in the previous research were repeated to reduce more complexities because changing everything or even referring to different literature would result in no solid grounds to support our research.

So, we selected NMP, PSS, and PVDF as the chemicals previously used (Gupta, 2016); however, changing the base material to CNP's supplied by Degussa (Germany), which are electrically conductive spherical particles.

## CHAPTER 3

### MATERIALS AND EXPERIMENTAL METHODOLOGY

#### 3.1 Materials

Following materials were used to develop conductive concrete. The characterization tests of these materials are also shown here. The overall experimental program is also discussed later in the chapter.

##### 3.1.1 Nano Material - Carbon Nano-particles (CNPs):

Carbon nanoparticles (CNPs) supplied by Degussa (Germany) were used. These particles have spherical geometry. As found through repeated and systematic investigations, the resulting polymer matrix composite becomes piezoresistive when the weight concentration of these nano-particles is maintained at 35 percent, as this concentration corresponds to the percolation threshold of these nano-particles,

Since CNPs are being added in addition to cement as well as being sprayed in one case, they can effectively serve the purpose of enhancement of mechanical properties and also forming an effective conductive network within the cementitious matrix for self-sensing purposes by having as fine the particle size as possible. Carbon Nanotubes (CNTs) have known to be effective in enhancing mechanical properties. Li et al. found that the addition of 0.5% multi-walled CNTs increased the Portland cement composite's compressive and flexural strength. Since they are nanoparticles, such a nano-reinforcement would delay the nucleation and growth of cracks on the nano-scale. If cracks are controlled at the nano-scale level, their propagation can be prevented to the micro-level (Babak et al., 2014). So to investigate the particles size and the morphology of CNPs, Scanning Electron Microscopy (SEM) was performed. SEM results are shown in figure 2 also complement this finding.



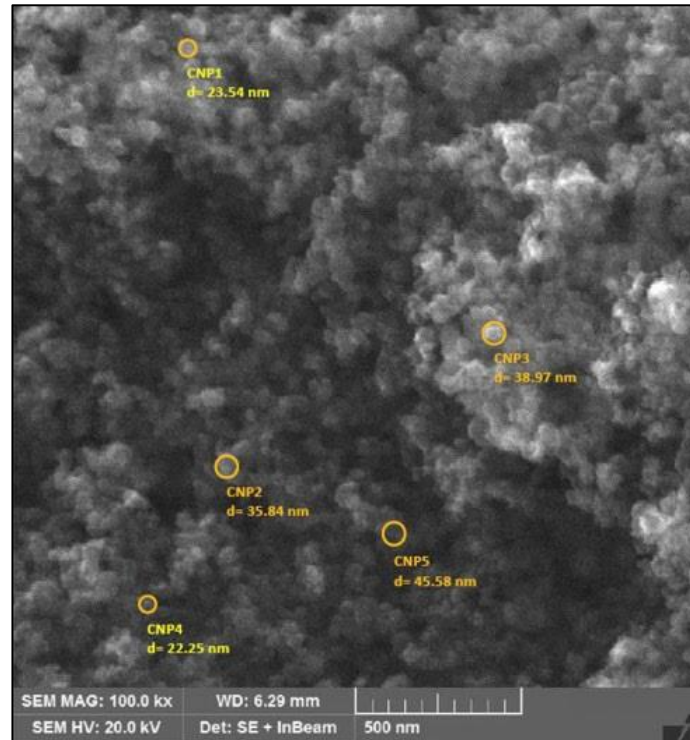


Figure 2: SEM image of Carbon Nano-Particles at 500 nm scale

This graph depicts the particle size range of CNPs. CNPs range in size from 10 to 58 nm in terms of overall percentage volume density. Particle volume density peaks between 18 and 25 nanometers, according to the data. Later, the same particles were examined using a MIRA3 TESCAN scanning electron microscope (Czech Republic) (SEM). The particle size analysis is supported by the image obtained from SEM, as the average particle size varies between 20 nm and 38 nm, as shown in Figure2.

### 3.1.2 N-Methyl-2-pyrrolidone (NMP)

Since it is known that nanoparticles having a high aspect ratio are difficult to disperse only through sonication. Therefore, different dispersing agents are used to disperse the nanoparticles in the concrete mix for this purpose. NMP is a well-known solvent for its capacity to disperse CNT at low concentrations (Terentjev, 2012). Our process of ink simulation consisted of making a 2% aqueous solution of PSS followed by the addition of a small amount of NMP to enhance dispersion, followed by the addition of CNPs, and then sonicated for 30 mins. The amount of NMP was determined by trial testing.

### 3.1.3 Poly sodium 4-styrene Sulfonate (PSS)

In order to make sure that the nanoparticles did not agglomerate, PSS was used as a surfactant. Previous research showed that PSS is capable of dispersing CNTs by noncovalent surface modifications. The CNTs dispersed with PSS were found to be highly dispersible in water.

The process involves making a 2% aqueous solution of PSS followed by adding a small amount of NMP to enhance dispersion, followed by the addition of CNPs and then sonicated for 30 mins. The amount of PSS was determined by trial testing.

SEM of PSS was carried out to check the morphology and structure of PSS. The results of SEM of PSS are shown in figure 3.

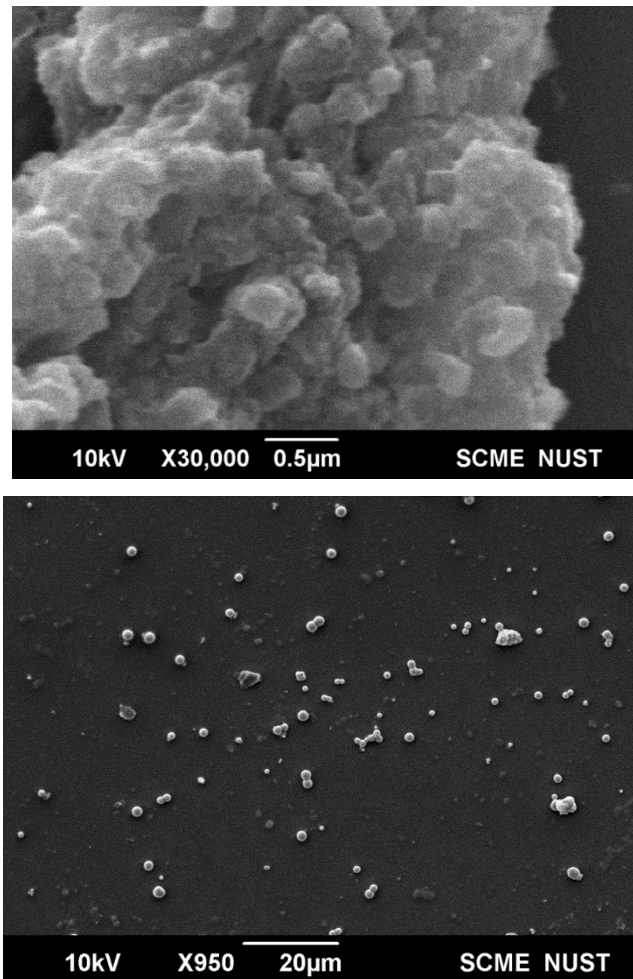


Figure 3: SEM of PSS at 0.5  $\mu$ m and 20  $\mu$ m scale

### 3.1.4 Polyvinylidene Fluoride (PVDF)

Since our main design consisted of coating the aggregate surfaces, for that purpose, the ink to be coated had to have adhesive properties. For this purpose, a small amount of PVDF was added after sonication, and the aggregates coated were subjected to air drying for 30 mins. The adhesive property of PDVF was confirmed by literature used to impart adhesive properties to CNTs ink (Gupta, 2016). PVDF is a highly inert specialty thermoplastic having a melting point of 175°C. It is produced by free-radical polymerization of 1,1-difluoroethylene (Voet, Vincent, 2014). The SEM results of PVDF are shown in figure 4.

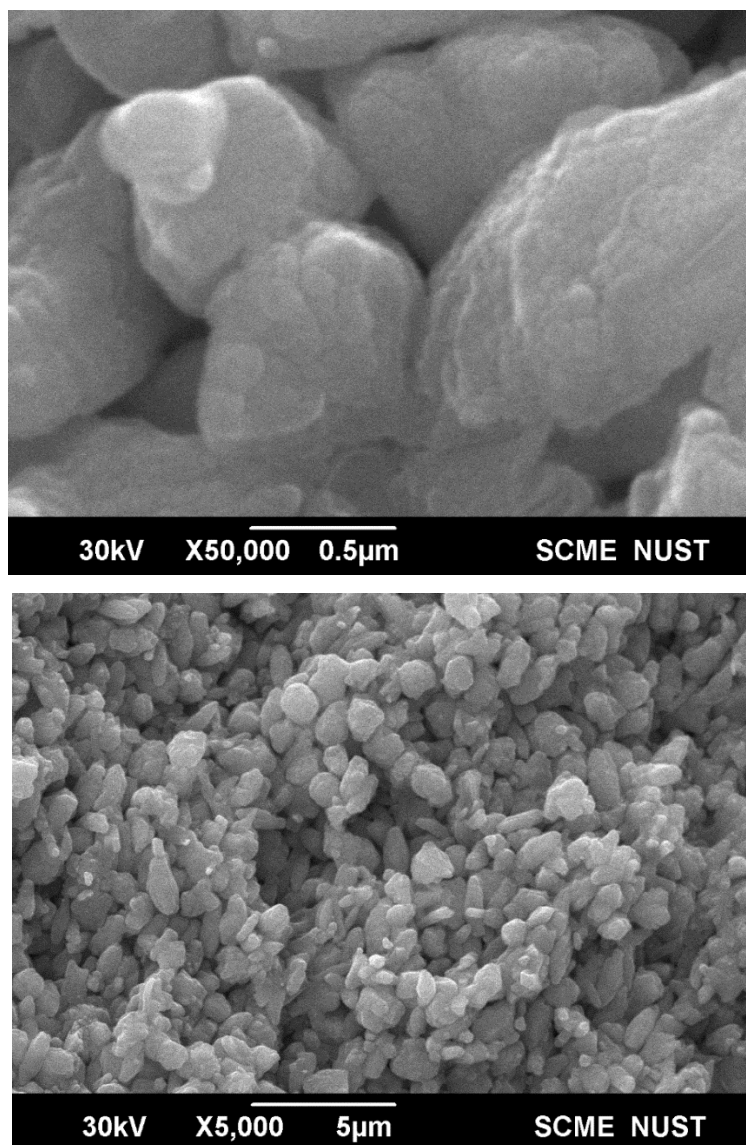


Figure 4: SEM of PVDF at 0.5 μm and 5 μm scale

### 3.1.5 Cement (Bestway)

Ordinary Portland cement was used as a binder in casting. Cement was kept in a sealed container to prevent any interaction with the atmosphere. Initially, the physical properties of the cement were determined, as shown in table 1.

Table 1: Cement properties

<b>Initial Setting Time</b>	162 mins
<b>Final Setting Time</b>	210 mins
<b>Normal Consistency</b>	27 %
<b>Blaine Fineness</b>	3650 cm <sup>2</sup> /gm
<b>Color</b>	Gray

### 3.1.6 Fine Aggregate

River Sand was procured from a local source. It is slightly fine to medium-sized sand. This was confirmed upon determining fineness modulus, which came out to be 3.184, within ASTM limits (2.2 to 3.2). Sieve analysis of the sand in accordance with ASTM C33 was done, and the gradation curve was plotted, as shown in figure 5. The gradation curve came out to be with the envelope specified by ASTM C33. Different properties of sand are shown in table 2.

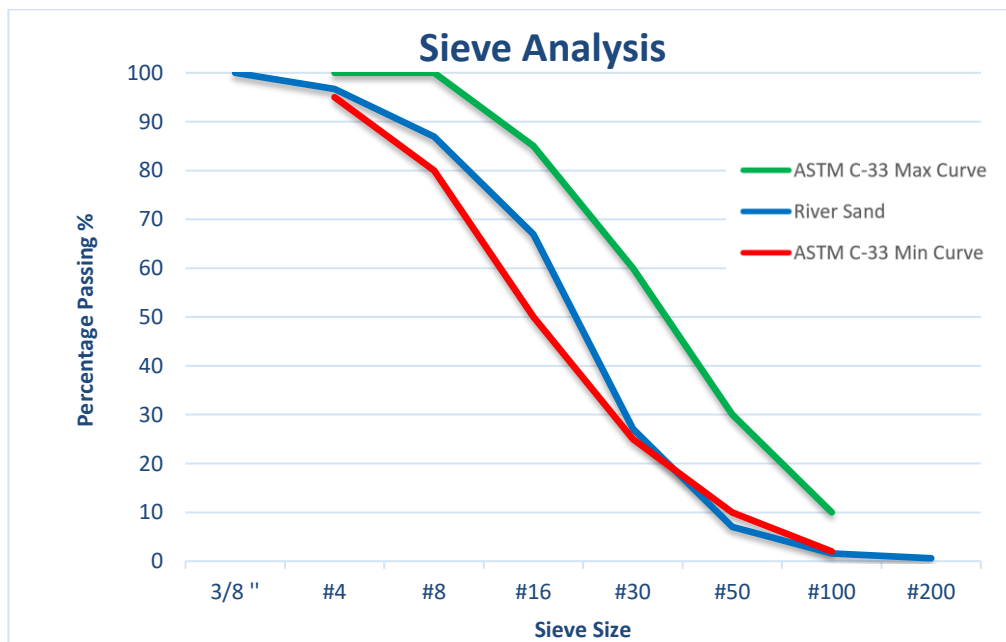


Figure 5: Particle Size Distribution of Sand

Table 2: Different properties of sand

<b>Median Size (D<sub>50</sub>)</b>	1 mm
<b>Absorption</b>	1.21 %
<b>Specific Gravity</b>	2.67 kg/m <sup>3</sup>
<b>Fineness Modulus</b>	3.184
<b>Passing Sieve</b>	3/8"

### 3.1.7 Coarse Aggregate

Margalla Crush Aggregate was used with a maximum nominal size of 19 mm. Different properties of aggregate are shown in table 3.

Table 3: Different properties of aggregate

<b>Maximum Nominal Size</b>	19mm
<b>Absorption</b>	1.04%
<b>Specific Gravity</b>	2.70 kg/ m <sup>3</sup>
<b>Abrasion Value</b>	26.04 %

### 3.1.8 Mixing Water

Water available in Structural lab, NICE was tested from IESE. The sample was found to be in accordance with WHO's (World Health Organization) guidelines and standards for portable use.

### 3.2 Experimental Methodology

In order to perform different types of tests on our multipurpose concrete, different sizes of concrete molds were cast. These included 152.4 x152.4 x 152.4 mm large Cubes and 4 x 8 in cylinders. In addition to these, for resistivity and damage sensing, cubes were cast with the insertion of 4x7 copper mesh plates.

The process of ink formation consisted of the preparation of 2% aqueous solution of PSS in deionized water, followed by the addition of CNPs to the solution. After that, a small amount of N-methyl-2-pyrrolidinone (NMP) was added to the mixture to enhance the dispersion of CNPs (see figure 7). Finally, the mixture was subjected to sonication for 30 mins at 25 degrees centigrade. Once the CNPs had achieved dispersion, the next step was to prepare a PVDF-based solution to be used for spray fabrication. PVDF was suspended in an aqueous surfactant solution and then diluted with water. The mixture was stirred vigorously to achieve dispersion. The ink fabrication process is illustrated in figure 6.

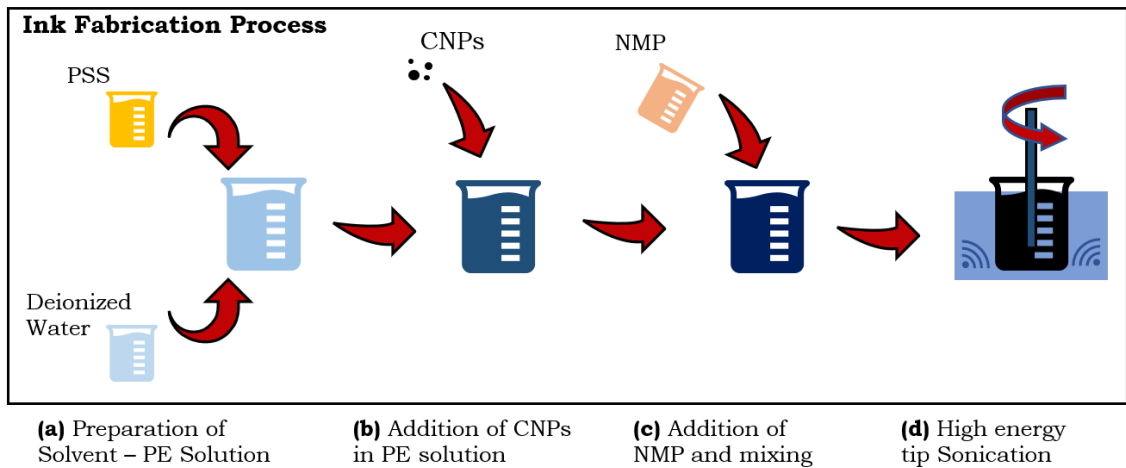


Figure 6: Ink Fabrication Process



Figure 7: Preparation of CNP based ink

The ink prepared was directly added to the concrete while mixing in additive concrete, as shown in figure 8.

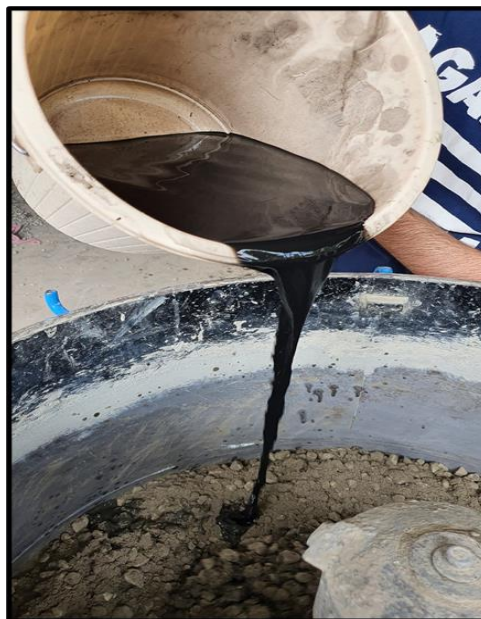


Figure 8: Addition of CNP Solution to Mix design

However, in sprayed conductive concrete, the ink formed was coated onto aggregate surfaces using an airbrush (figure 9). Coarse aggregates were mixed with a spatula to expose uncoated aggregates, and the spraying was repeated. To get a uniform coating, sand required twice as much ink as coarse aggregates (figure 10). A total of 6 coatings were applied on the sand and three coatings on coarse aggregates. After uniform coating was achieved, the treated aggregates were air-dried for 60 mins before using them in casting concrete samples.



Figure 9: Coarse aggregate before and after coating



Figure 10: Fine aggregates before and after spray

### 3.2.1 Optimum Proportion & Sonication

The research gap of this research lay in determining the optimum quantities of materials required to make a uniform conductive ink that could disperse the CNPs effectively. Hence, to determine optimum quantities of chemicals such as NMP and PSS, we had to carry out trial tests in 100ml solution and later dilute them to get desired results. A total of four ratios were used to check the optimum concentration of these materials, which would provide the best dispersion of CNPs in ink. Also, sonication time was noted for all four ratios, and the most optimum time was chosen.

The testing procedure consisted of making NMP based solution of CNPs in a test tube, and later a PSS-deionized water solution was prepared and mixed into the



NMP-CNPs based solution. Both NMP and PSS were added to enhance the dispersion of CNPs. After that, the solution was subjected to hip tip bath sonication.



Figure 11: Sonication in Progress, Glass test tubes having different proportions

After sonicating the different mixes, a spectrophotometer was used to check the absorption at 600nm because the max absorption wavelength for our solution was around 600nm. The trial with the highest absorption was said to be the most well-dispersed solution, followed by optimum sonication time as well.



Figure 12: Spectrophotometer, Peak Detection Values

After a series of trials, the optimum ratio of NMP-PSS was found to be 50/50, followed by a sonication time of 30 mins. The results of trials carried out are shown in table 4.

Table 4: Trials for optimum proportion of solution constituents

<b>Spectrophotometer Absorbance @ 600nm</b>				
	<b>PSS/NMP Proportion</b>			
<b>Sonication Time (min)</b>	<b>80/20</b>	<b>70/30</b>	<b>50/50</b>	<b>30/70</b>
15	0.351	0.46	0.578	0.379
30	0.398	0.474	<b>0.596</b>	0.529
45	0.363	0.476	0.501	0.502

### 3.2.2 Mix Design

ACI mix design procedure was implemented, and mix proportions shown in table 5 were finalized for all concrete types. No superplasticizer was used in casting. Cement sand aggregate ratio of 1: 1.64:2.47 was finalized.

Table 5: Mix Design

<b>Specimens</b>	<b>Unit</b>	<b>Control</b>	<b>Additive</b>	<b>Spray</b>
<b>Cement</b>	kg/m <sup>3</sup>	400	400	400
<b>Sand</b>	kg/m <sup>3</sup>	1550	1550	1550
<b>Aggregate</b>		1650	1650	1650
	kg/m <sup>3</sup>			
<b>W/C Ratio</b>		0.48	0.48	0.48
<b>CNPs</b>	% w.r.t Cement	-	0.065	0.065
<b>Ink Incorporation Technique</b>		-	Direct as additive	By Spraying on Aggregates

### 3.2.3 Mixing Regime

Pan mixer was used to mix all materials to get a homogenous mix. Literature has suggested that the minimum time a composite cementitious material takes to mix effectively within the cementitious matrix is within 2 to 5 minutes. So based on our trial casting, a 3-minute mixing regime was finalized. Initially, slow dry mixing (145 rpm) of cement and sand was carried out for 30 seconds. Then 85% of the total water and 100% of both CNPs and PVDF was added to the dry mix, and then slow wet mixing was carried out for 60 seconds, after which remaining water containing remnants of CNPs was added, and fast wet mixing (285 rpm)

was carried out for 90 seconds. Detailed steps of mix preparation have been tabulated in table 6.

Table 6: Execution steps of casting

<b>Step 1</b>	Sonicate 85% of total water containing CNPs and for at least 30 minutes prior to the start of any mixing, at around 25°C.
<b>Step 2</b>	Slow dry mix cement, sand for 30 seconds.
<b>Step 3</b>	Take sonicated solution out of sonicator and wait 2-3 minutes for the temperature to decrease slightly.
<b>Step 4</b>	Once steps 2 and 3 ends, add the sonicated solution in dry mixed solution and carry out 60 seconds of slow wet mixing.
<b>Step 5</b>	Once step 4 ends, using the remaining 15% of water.
<b>Step 6</b>	Fast wet mix for 90 seconds
<b>Step 7</b>	Cast the prepared material in molds.

### 3.2.4 Slump Test

The Slump test (ASTM C 143) was carried out for all three mix designs to check the effect of CNPs addition on the slump value. All three designs had almost the same slump of 75mm, which showed no effect of either CNPs coating and addition on the concrete slump. As shown in figure 13 below, the three mix designs are control concrete, additive concrete, and sprayed concrete.



Figure 13: Slump (Control, CNP as additive, CNPs Sprayed)

### **3.2.5 Curing Process**

Samples were placed in water for curing, at room temperature, for a standard period of 28 days for most of the tests before they were removed for testing. Samples were demolded 24 hours of casting.

## EXPERIMENTAL TESTS AND RESULTS

### 4.1 Modulus of Rupture (MoR)

Modulus of Rupture or MoR values of each specimen tested can be directly obtained from UTM as shown in figure 14 or can be calculated by determining yield stress and putting it into the following equation;

$$MoR = 3PL/2bd^2$$

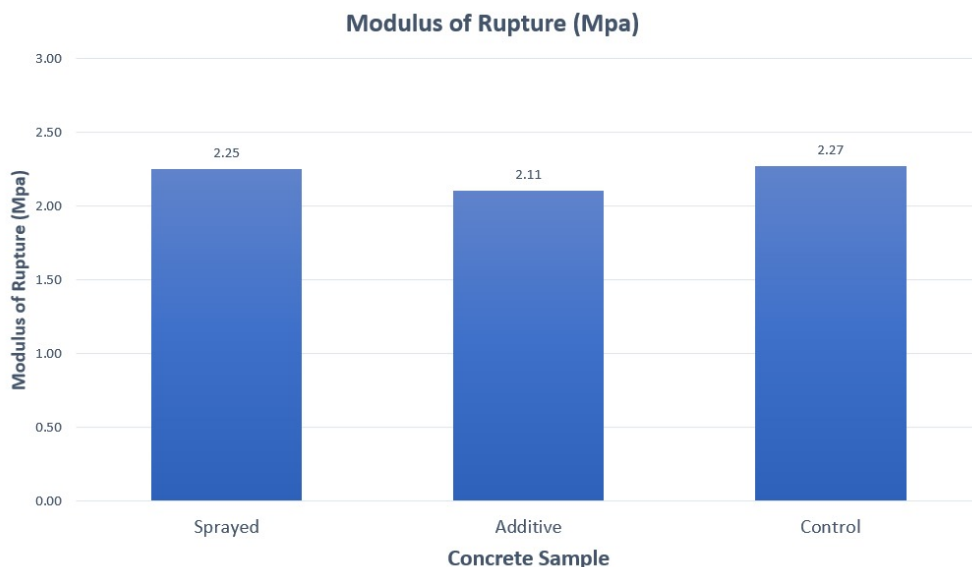


Figure 14: Modulus of rupture values

The results show that there is a slight variation between the MoR values of the three mixes. The effect of CNPs, either as an additive or spray, impart a slight reduction in the MoR value of the concrete samples. Control has the highest value of MoR since there is no addition to the concrete morphology, whereas sprayed concrete has almost the same MoR as Control which shows no detrimental effect of the spray film on the concrete strength. Additive, however, shows a slight reduction in MoR, which may happen due to flake formation in the cement mix due to CNPs ink being directly added (Zdeněk P. 1995)

## 4.2 Compressive Strength

Compression test was performed at a stress rate of 0.25 MPa/sec as per ASTM C 109. Specimens were tested after 28 days of curing. Flexural strength has to be around 10- 15% of the compressive strength according to the convention, which has been verified by our compression results, as shown in figure 16.



Figure 15: Compressive Strength Test Cylinder in UTM

A similar trend for compressive strength in comparison to MoR was achieved. The two ways of CNPs addition to the concrete mix affected the compressive strength negatively, reducing the compressive strength but in an acceptable manner. Control had the highest value of compressive strength, around 26 MPa, whereas sprayed concrete had a slight reduction of around 24 MPa, and additive concrete showed the lowest strength, around 21.5 MPa.

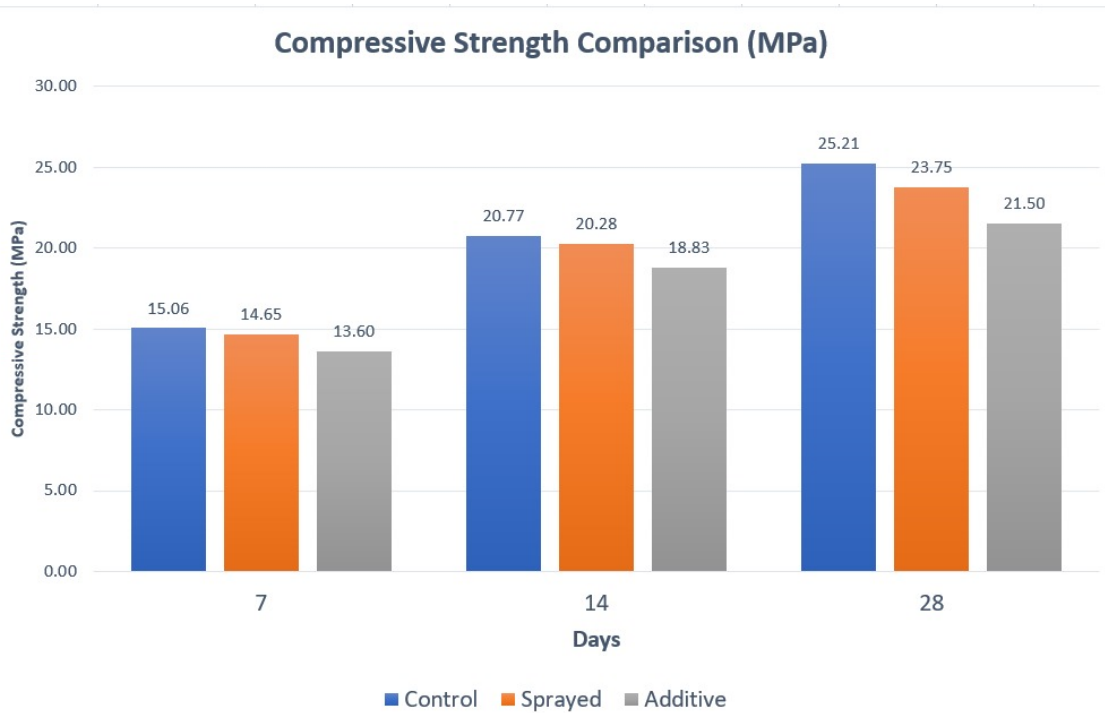


Figure 16: Compressive strengths and comparison with MoR

The reason being that CNPs being sprayed on the aggregate surfaces lowers the ITZ bond and thus, with time, lowers the strength and bond formation. This trend is also evident from 7-, 14- and 28-day strength comparison, as shown in figure 16. Whereas, on the contrary, the additive method of CNPs results in the formation of flakes in the cement mix over time, resulting in strength reduction to the most (Zdeněk P. 1995).

### 4.3 Bulk Resistivity

Bulk resistivity uses a two-point technique, such that two electrodes are used to send and read the current flow in a concrete sample. The test consists of a digital resistivity array meter, thin metal plates, and sponges. Wet sponges are attached to both sides of the cylinder, and metal plates are placed on them. The probe of the array meter is attached to the sponge on the bottom, and reading is taken directly by touching the other probe to the top plate. The test setup is shown in figure 17 below:



Figure 17: Bulk Resistivity Test

Results show that the resistivity values of concrete decrease effectively by the addition of CNPs into the concrete. Sprayed concrete showed the lowest values of resistivity, which strengthened the idea that a dense conductive path is formed when you coat the aggregate surface with conductive materials, whereas normal addition also showed a reduction in the resistivity values but lesser effective than sprayed due to the fact the quantity of CNPs used was less and might not have reached the percolation threshold. However, this was not our concern as it was to be a comparative study. To conclude, sprayed concrete showed a nearly 45%



reduction in resistivity compared to control concrete, whereas the additive method only showed only 15-20% reduction in resistivity. Hence, sprayed concrete was believed to be more sensitive to changes in resistivity than additive and control concrete. The comparison of resistivity values calculated by the bulk resistivity is shown in figure 18 below:

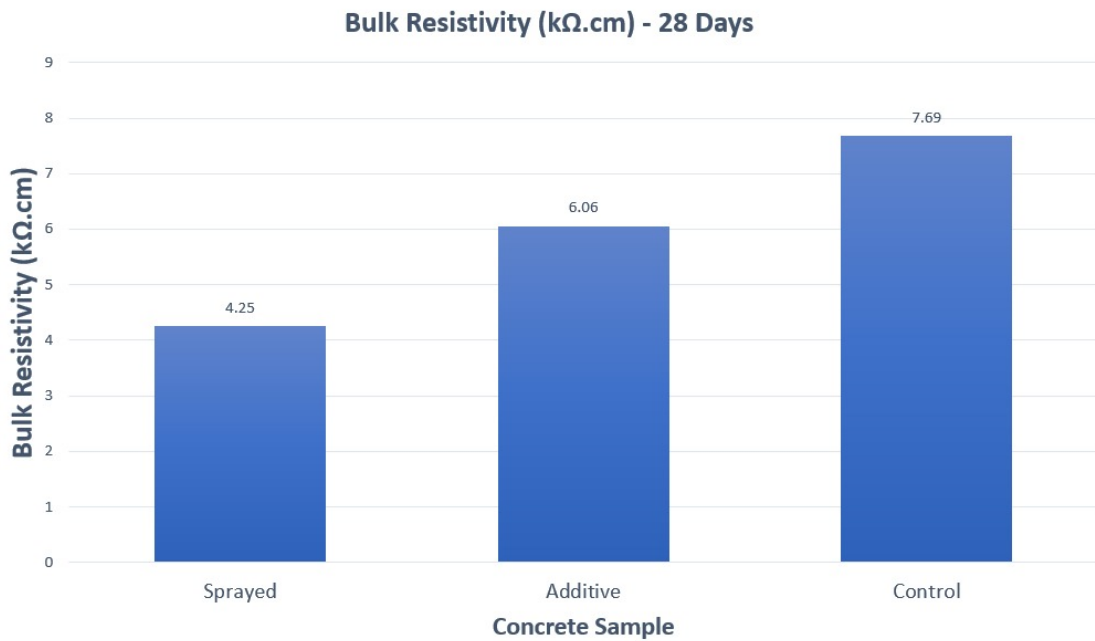


Figure 18: Bulk Resistivity Test Result

## **4.4 Self-Sensing**

### **4.4.1 Test setup and procedure**

All electrical conductivity tests in the lab trial have been carried out using the 2-probe technique, where only sample types were changed based on the type of test. The general procedure of this technique involves intruding two copper plates or wrapping copper films based on sample type (prism or cube), which serve as probes/terminals to apply voltage via the power supply and record voltage drop and current passed.

The voltage supply is connected to the probes, and the current passed while voltage drop is measured at probes. The apparatus devised for this test includes 25V, with frequency 1 kHz whereas current was between 0.1-10 mA, voltage source and two multi-meters to record voltage drop and current passed simultaneously.

Resistance is then measured by Ohm's law formula:

$$V = IR$$

Where V is the voltage drop recorded and I being the current passed. The resistivity of the sample is then measured by using the formula:

$$R = \rho L / A$$

where L is the distance between two inner probes and A is the cross-sectional area.

### **4.4.2 Piezoresistive Test – Damage Sensing (DS)**

To develop self-sensing property, it is of paramount importance to study the response of resistivity of test specimens with respect to loading applied. This type of testing is called piezoresistive testing. The most important domain in piezoresistive testing is damage sensing.

In this test, the resistivity response is evaluated with respect to the ultimate failure load. The test specimens used for this test were 150x150 mm mortar cubes. Two copper. The resistivity was being recorded using the 2- Probe technique under live compressive loading by UTM at a rate of 0.05 Mpa/sec. Figure 19 shows the experimental setup for the piezoresistive test.

(a)



(b)



(c)



Figure 19: Piezoresistive Testing apparatus Setup

The results shown in figure 20 indicate that resistivity has an indirect relationship with an increase in load. This is because, with the increase in load, the distance between CNPs decreases along the direction of load application, which results in the development of more conductive paths, hence decreasing resistivity.

However, the decrease in the initial loading phase is more as compared to when substantial loading has been applied. This is due to the reason that in the initial phase, resistivity is being decreased due to not only the inter-particle distance of the CNPs being decreased but also the voids being reduced. Whereas, in the second near linearly decreasing phase maximum number of voids has already been reduced due to a substantial density increase in the first phase.

On the other hand, when we compare the resistivity curves of different mixes, the curve for the sprayed concrete has a greater slope as compared to the other two, showing greater sensitivity to load being applied and a more defined conductive path. However, the additive has a relatively smooth curve throughout, which decreases with the applied load as the particle distance decreases. Control concrete has the greatest resistance and lesser effect on resistivity by the load being applied to it.

When the load value approaches the ultimate failure load, resistivity shoots to infinity. This is due to breakage of conductive path caused by extensive cracking.

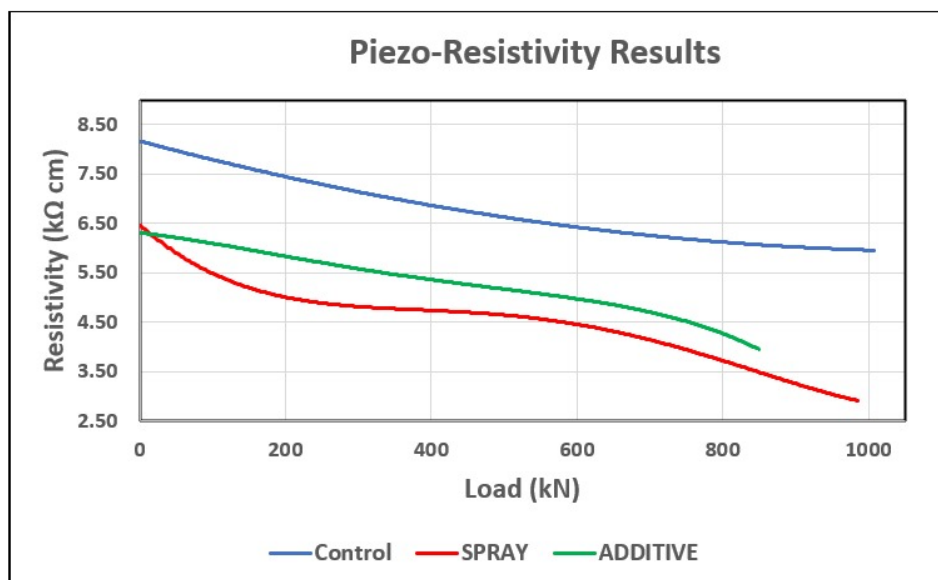


Figure 20: Resistivity vs. Load trend in damage sensing

## CHAPTER 5

### CONCLUSIONS

The following conclusions are drawn based upon the results;

1. NMP/PSS optimum proportions were found to be **1:1**
2. Optimum sonication time for CNPs in NMP/PSS solution was found to be **30 minutes**
3. SEM average particle size of CNP was found to be **(20 – 38) nm**
4. Airbrushing technique showed an almost **50%** reduction in resistivity compared to control normal concrete.
5. Airbrushing technique showed an almost **27%** reduction in resistivity compared to the conventional (additive) technique.
6. Compressive strength is comparable but slightly less by **5%** compared to control concrete, which is within safe limits.
7. Airbrushing technique shows a more sensitive response to change in resistivity with the application of load (Damage Sensing) as compared to additive technique and control concrete readily

## **RECOMMENDATIONS**

- 1- Analyze the effects of curing age on the resistivity of the nano-engineered concrete and identify the time after which resistivity becomes constant.
- 2- Investigate ways to cater to the durability concerns attached to the fact that lowering the concrete resistivity increase corrosion potential.
- 3- Analyze water content effects on resistivity and piezoresistivity.
- 4- Study effect of superplasticizers to cater for the strength reduction in nano-engineered concrete.
- 5- Design data relay equipment and software interface to interpret the data received and strategies to use this system in SHM applications.
- 6- Study nano-engineered concrete performance at elevated temperatures.

## REFERENCES

- Banthia N, Djeridane S and Pigeon M. Electrical resistivity of carbon and steel micro-fiber reinforced cements. *Cement Concrete Res* 1992; 22: 804–814.
- Banthia N and Sheng J. Micro-reinforced cementitious materials. In: *Proceedings for the 1990 MRS Fall Meeting & Exhibit*, Boston, MA, 26 November–1 December 1990, pp. 25–32. Cambridge University Press.
- Ding Y, Han Z, Zhang Y, et al. Hybrid use of steel and carbon-fiber reinforced concrete for monitoring of crack behavior. In: *15th European conference on composite materials (ECCM15)*, Venice, Italy, 24–28 June 2012, pp. 1–8, European Society For Composite Materials.
- Chen P-W and Chung D. Carbon fiber reinforced concrete as an intrinsically smart concrete for damage assessment during static and dynamic loading. *ACI Mater J* 1996; 93: 341–350.
- Loh KJ and Gonzalez J. Cementitious composites engineered with embedded carbon nanotube thin films for enhanced sensing performance. *J Phys Conf Ser* 2015; 628: 012042.
- Ding Y, Chen Z, Han Z, et al. Nano-carbon black and carbon fiber as conductive materials for the diagnosing of the damage of concrete beam. *Constr Build Mater* 2013; 43: 233–241.
- Gupta S, Gonzalez J and Loh K. Damage detection using smart concrete engineered with nanocomposite cement aggregate interfaces. In: *10th international workshop on structural health monitoring*, Stanford, CA, 1–3 September 2015, pp. 3033–3041. Destech Publications, Inc.
- Yu X and Kwon E. A carbon nanotube/cement composite with piezoresistive properties. *Smart Mater Struct* 2009; 18(055010): 1–5.
- Ma P-C, Siddiqui NA, Marom G, et al. Dispersion and functionalization of carbon nanotubes for polymer-based nanocomposites: a review. *Compos Part A: Appl S* 2010; 41: 1345–1367.

Ackermann, Kay Christian, "SELF-SENSING CONCRETE FOR STRUCTURAL HEALTH MONITORING OF SMART INFRASTRUCTURES" (2018). Open Access Master's Theses. Paper 1285.

Screen-printed nanocomposite sensors for online in situ structural health monitoring - Taimoor A Khan, Saad Nauman, Zeeshan Asfar, M Ali Nasir, Zaffar M Khan, 2020 (sagepub.com)

On the in-situ on-line structural health monitoring of composites using screen-printed sensors - Saad Nauman, Zeeshan Asfar, Sheraz Ahmed, M Ali Nasir, Nourredine Aït Hocine, 2021 (sagepub.com)

Self-sensing concrete enabled by nano-engineered cement-aggregate interfaces - Sumit Gupta, Jesus G Gonzalez, Kenneth J Loh, 2017 (sagepub.com)

Lu, S., Xie, N., Feng, L., & Zhong, J. (2015). Applications of Nanostructured Carbon Materials in Constructions: The State of the Art. *Journal of Nanomaterials*, 2015, 1– 10. <https://doi.org/10.1155/2015/807416>

Sini Bhaskar 2016, Self-Healing Bacterial Cementitious Concrete Composites: Development and Performance Evaluation

Seung-Jung Lee, Ilhwan You, Goangseup Zi and Doo-Yeol Yoo, 2017, Experimental Investigation of the Piezoresistive Properties of Cement Composites with Hybrid Carbon Fibers and Nanotubes

Sardar Kashif Ur Rehman, Zainah Ibrahim, Mohammad Faisal Javed and Mohammad Usman Hanif, 2017, Piezo-Resistive Characteristics of Graphene-Based Cement Materials

Zuo, J., Yao, W., Liu, X., & Qin, J. (2013). Sensing Properties of Carbon Nanotube – Carbon Fiber / Cement Nanocomposites, 40.

Junjie Wang, Sreejith V. Nanukuttan, P. A. Muhammed Basheer, 2014, Influence of Micro and Macro Cracks Due to Sustained Loading on Chloride-Induced Corrosion of Reinforced Concrete Beams



Determining the Electrical Resistivity of Hardened Concrete Using Different Specimen Geometry Factors, Electrode Configurations, and Electric Currents (researchgate.net)

Full article: Direct dispersion of SWNTs in highly conductive solvent-enhanced PEDOT:PSS films (tandfonline.com)

Stabilization and “Debundling” of Single-Wall Carbon Nanotube Dispersions in N-Methyl-2-pyrrolidone (NMP) by Polyvinylpyrrolidone (PVP)

Guadalupe Sierra-Beltran, M., Jonkers, H.M., and Schlangen, E., (2014), “Characterization of sustainable bio-based mortar for concrete repair”, *Construction and Building Materials*, Vol. 67, No. 9, pp. 344–352.

Achal, V., Mukherjee, A. And Reddy, M.S., (2011a), “Microbial concrete: A way to enhance the durability of concrete buildings”, *Journal of Materials in Civil engineering*, Vol. 23, No.6, pp. 730-734.

Tian, L., Meziani, M. J., Lu, F., Kong, C. Y., Cao, L., Thorne, T. J., & Sun, Y. P. (2010). Graphene oxides for homogeneous dispersion of carbon nanotubes. *ACS Applied Materials and Interfaces*. <https://doi.org/10.1021/am100687n>

A. Celzard, E. Mcrae, C. Deleuze, M. Dufort, G. Furdin and J. Mareche, "Critical concentration in percolating systems containing a high-aspect-ratio filler," *Phys Rev B*, vol. 53, no. 10, pp. 6209-6214, 1996.

Babak, F., Abolfazl, H., Alimorad, R., & Parviz, G. (2014). Preparation and mechanical properties of graphene oxide: cement nanocomposites. *The scientific world journal*, 2014, 276323. <https://doi.org/10.1155/2014/276323>

Dr. Xun Yu, Dr. Eil Kwon, 2012, Carbon Nanotube Based Self-sensing Concrete for Pavement Structural Health Monitoring

Seung-Jung Lee, Ilhwan You, Goangseup Zi and Doo-Yeol Yoo, 2017, Experimental Investigation of the Piezoresistive Properties of cement Composites with Hybrid Carbon Fibers and Nanotubes.

Dr. Koushik Roy, Dr. Suparno Mukhopadhyay, 2016, Earthquake Resistance Of Low- Cost Engineered Housing In North-East India.

Andrea Meoni , Antonella D'Alessandro , Austin Downey , Enrique García-Macías , Marco Rallini , Rafael Castro- Triguero and Filippo Ubertini, 2018, An Experimental Study on Static and Dynamic Strain Sensitivity of Embeddable Smart Concrete Sensors Doped with Carbon Nanotubes for SHM of Large Structures.

M. Sun, W. J. Staszewski, and R. N. Swamy, 2009, Smart Sensing Technologies for Structural Health Monitoring of Civil Engineering Structures.

LI Hui, OU Jinping, 2011, Structural Health Monitoring: From Sensing Technology Stepping to Health Diagnosis

Faezeh Azhari, Nemkumar Banthia, 2012, Cement-based sensors with carbon fibers and carbon nanotubes for piezoresistive sensing.

Forood Torabian Isfahani (2016), Effects of Nanosilica on Compressive Strength and Durability Properties of Concrete with Different Water to Binder Ratios

Moubray, J. Reliability Centered Maintenance II, 2nd ed.; Butterworth-Heinemann: Oxford, UK, 1997; ISBN 0760633581.

Toward Structural Health Monitoring of Civil Structures Based on Self-Sensing Concrete Nanocomposites: A Validation in a Reinforced-Concrete Beam

Castañeda-Saldarriaga, D.L., Alvarez-Montoya, J., Martínez-Tejada, V. et al. Toward Structural Health Monitoring of Civil Structures Based on Self-Sensing Concrete Nanocomposites: A Validation in a Reinforced-Concrete Beam. *Int J Concr Struct Mater* 15, 3 (2021).

Nauman, S. Piezoresistive Sensing Approaches for Structural Health Monitoring of Polymer Composites—A Review. *Eng* 2021, 2, 197-226

Voet, Vincent & ten Brinke, G. & Loos, Katja. (2014). Well-Defined Copolymers Based on Poly(vinylidene fluoride): From Preparation and Phase Separation to Application. *Journal of Polymer Science Part A: Polymer Chemistry*. 52. 10.1002/pola.27340.

Modulus of Rupture: Size Effect due to Fracture Initiation in Boundary Layer  
Zdeněk P. Bažant

Artamonova, O.V., Slavcheva, Chernyshov. E.M. Effectiveness of combined nanoadditives for cement systems. *Inorganic Materials*. 2017. Vol. 53